



HAL
open science

Natural radionuclides ^{210}Po and ^{210}Pb in the Delaware and Chesapeake Estuaries: modeling scavenging rates and residence times

D. Marsan, T. Church, Sylvain Rigaud

► **To cite this version:**

D. Marsan, T. Church, Sylvain Rigaud. Natural radionuclides ^{210}Po and ^{210}Pb in the Delaware and Chesapeake Estuaries: modeling scavenging rates and residence times. *Journal of Environmental Radioactivity*, 2014, 138, pp.447-455. 10.1016/j.jenvrad.2014.08.014 . hal-01717777

HAL Id: hal-01717777

<https://hal.science/hal-01717777v1>

Submitted on 26 Feb 2018

HAL is a multi-disciplinary open access archive for the deposit and dissemination of scientific research documents, whether they are published or not. The documents may come from teaching and research institutions in France or abroad, or from public or private research centers.

L'archive ouverte pluridisciplinaire **HAL**, est destinée au dépôt et à la diffusion de documents scientifiques de niveau recherche, publiés ou non, émanant des établissements d'enseignement et de recherche français ou étrangers, des laboratoires publics ou privés.

2 **Natural Radionuclides ²¹⁰Po and ²¹⁰Pb in the Delaware and Chesapeake Estuaries; Modeling**
3 **scavenging rates and residence times**

4 Marsan, D., Rigaud, S., and Church, T.

6 School of Marine Science and Policy, University of Delaware, Newark, DE 19716-3501 USA.

8
10 Journal of Environmental Radioactivity

12
14
16
18
20 Corresponding author

David Marsan

22 dmarsan@udel.edu

Phone: (908) 268-9204

24 Present Address:

013Lammot DuPont Laboratory

26 Newark, DE 19711 USA

28 Sylvain Rigaud

30 s.rigaud@epoc.u-bordeaux1.fr

Thomas Church

32 tchurch@udel.edu

Natural Radionuclides ^{210}Po and ^{210}Pb in the Delaware and Chesapeake Estuaries; Modeling scavenging rates and residence times

50

52

54

Highlights

56

1) Estuarine ^{210}Pb and ^{210}Po data reveal key biogeochemical processes and rates

58

2) Delaware Bay displays regional differentiation due to dominant particle reactions

58

3) Chesapeake Bay displays vertical differentiation from deep sub-oxic redox cycling

60

4) Parent (^{210}Pb) grand-daughter (^{210}Po) disequilibria evidence principle processes

60

5) Net scavenging residence times calculated weeks (Delaware) to months (Chesapeake)

62

64

66

68

70

72

74

76

78

80

82

84

86

88

90

92

94

96

Abstract

98 During the spring and summer months of 2012, ^{210}Po and ^{210}Pb activity were
measured in the dissolved and particulate phases from the Delaware and upper Chesapeake
100 estuaries. Both nuclides were also determined in the dissolved phase during a tidal cycle
from a lower Delaware salt marsh. The upper Delaware estuary, near the freshwater end
102 member, was characterized by high-suspended matter concentrations that scavenged
dissolved ^{210}Po and ^{210}Pb . The intertidal marsh acted as a source for dissolved ^{210}Po and
104 ^{210}Pb to the Delaware estuary, while deeper within the marsh evidence of bioaccumulation
and remineralization of ^{210}Po was observed. Box models were applied using mass balance
106 calculations to assess the nuclides residence times in each estuary. A consecutively
sectioned (upper, mid, and lower) box-model of the Delaware estuary found the mean
108 dissolved scavenging residence time of ^{210}Po to be relatively constant (20-25 days)
throughout all of the sections. However, dissolved ^{210}Pb scavenging residence times
110 decreased from 21 to 10 days from the upper to lower estuary. Only 60% of the dissolved
 ^{210}Po and 55% of the dissolved ^{210}Pb from the Delaware estuary were exported to coastal
112 waters. A large fraction of soluble ^{210}Po and ^{210}Pb within the estuary was either reversibly
adsorbed onto suspended particles or trapped in sediment accumulation zones (such as
114 intertidal marshes), or bioaccumulated by phytoplankton and discharged to the coastal
ocean. The upper Chesapeake estuary was largely characterized by sub-oxic bottom waters
116 that contained higher concentrations of dissolved ^{210}Po and ^{210}Pb , hypothesized to be
subjected to redox cycling of manganese. The Delaware and Chesapeake estuary mean
118 residence times for ^{210}Po differed significantly at 87 and 126 days respectively, while they
were similar for ^{210}Pb (53-67 days). The difference in residence times corresponds to the
120 greater extent of biogeochemical scavenging and regeneration processes within the upper
Chesapeake.

Keywords

124 ^{210}Po ; ^{210}Pb ; estuaries; salt marsh; Anoxic; Chesapeake Bay; Delaware Bay

126

128 **1 Introduction**

130 Estuaries are among the most important regions for the transfer of continental
132 dissolved and particulate elements to the oceans (Millward and Turner, 1995). These
134 elements enter the estuarine system via rivers from natural weathering of continental
136 material, anthropogenic discharges from urban areas, groundwater, and atmospheric
138 fallout. In the estuarine region, the elements are subjected to a series of biogeochemical
140 processes in the water and sediments, which include adsorption, transformation,
uptake/release by estuarine microorganisms, and removal by biogeochemical scavenging.
These processes can result in significant modification of the transfer fluxes from the
continent to the oceans. Such transfers associated within the estuarine river and seawater-
mixing zone are well established (Church, 1986). However, the rates are difficult to
establish without the use of radionuclide tracers to help understand and quantify the
changes.

Over the past several decades, the naturally occurring radionuclide pair of ^{210}Po and
 ^{210}Pb has been widely used to examine dissolved and particle dynamics in open ocean
ecosystems (Bacon et al., 1976; Nozaki, et al. 1976; Thomson and Turekian, 1976; Cochran
and Masque, 2003; Rutgers van der Loeff and Moore, 2007). The systems controlling ^{210}Po
and ^{210}Pb dynamics in the ocean are relatively well constrained and mainly associated with
sorption onto particles (^{210}Pb) and biogenic material cycling (^{210}Po). However, in coastal
and estuarine systems these dynamics are less constrained due to high temporal and spatial
variability. Indeed, estuarine and coastal waters are subjected to seasonal changes of water
flow, particle re-suspension/transport from different origins, eutrophication,
phytoplankton bloom events, exchange with the ocean, and anthropogenic inputs that
influence ^{210}Po and ^{210}Pb dynamics. In addition, ^{210}Po and ^{210}Pb radionuclides have several
origins in coastal environments. Sources include riverborne sediment (Chung and Chang,
1995; Smoak et al., 1996; Santschi et al., 1979), boundary scavenging of ^{210}Pb (Bacon et al.,
1976; Chung and Chang, 1995; Smoak et al., 1996), or regeneration of ^{210}Po from rapidly
degrading biogenic particles or upwelling (Heussner et al., 1990).

Several studies have used the ^{210}Pb and ^{210}Po nuclide pair in the estuarine marine
environment as quantitative tracers (Benninger, 1978; Santschi et al., 1979; Church, 1986;
Church and Sarin, 1995; Carvalho, 1997). From this limited research, it has been verified
that removal of these nuclides are primarily controlled by the particulate matter
concentration (Santschi et al., 1979) and with nuclide disequilibria imposed along the
seasonal salinity gradient, which is due to particle scavenging along these gradients (Church

162 and Sarin, 1995). Estuarine environments are also subject to hypoxic/anoxic conditions
with specific biogeochemical dynamic at redox interfaces that clearly impact the ^{210}Po and
164 ^{210}Pb dynamics in the ocean (Bacon et al., 1980; Wei and Murray, 1993; Kim et al., 2005). It
was shown that within anoxic basins scavenging of radionuclides by Fe and Mn rich
166 particulate matter and by bacteria affects distribution in the water column.

This paper presents a comprehensive estuarine data set on the radionuclides ^{210}Po
168 and ^{210}Pb for two of the largest U.S. estuaries, the Delaware and Chesapeake (Figure 1). Both
estuaries receive major fresh water input, the Delaware and Susquehanna Rivers, which
170 host the metropolitan regions of Philadelphia and Baltimore, respectively. The Delaware
River is shallow, with an average depth of 10m, and bordered by numerous intertidal creeks
172 and salt marshes. The upper Delaware estuary has a well-defined turbidity maximum, and
during the spring, bloom events occur within the lower estuary. In contrast, the Chesapeake
174 Bay is a composite of several smaller river-estuarine systems, each with individual
lithologies and drainage characteristics. The section north of the Potomac (Figure 1) is a
176 deep drowned river channel sided by clay cliffs that often contain basins of suboxic to
anoxic conditions at depth during the summer time. On average, the Delaware estuary has a
178 flushing time averaging 3 months, while the upper Chesapeake flushing can range from 6-12
months. Both estuaries are commensurate with the ^{210}Po half-life (138days) and thus
180 compatible with the $^{210}\text{Po}/^{210}\text{Pb}$ radionuclide parent-daughter pair (Church and Sarin,
1995). These estuaries present two distinct biogeochemical systems and provide an overall
182 rationale to use the ^{210}Po and ^{210}Pb radionuclides to better understand and quantify
processes controlling the fate and behavior of other proxy trace elements in estuarine
184 environments.

Here we report data on ^{210}Po and ^{210}Pb activities in the dissolved and particulate
186 phases along the salinity gradients of the Delaware and upper Chesapeake estuary. This
data is supported by physiochemical water parameters: temperature, salinity, dissolved
188 oxygen, fluorescence, suspended matter, particulate organic carbon (POC) and nitrogen
(PON), and major nutrients (NO_3^- , NH_4^+ , PO_4^{3-} and Si) concentrations. The main objectives of
190 this paper are to 1) improve understanding of ^{210}Po and ^{210}Pb cycling in the estuarine
environment, 2) use the radionuclide pair to quantify dissolved-particulate exchange rates
192 that translate to scavenging residence times 3) assess the potential role of pervasive
intertidal salt marshes that may contribute to the nuclide distribution of the lower
194 Delaware Bay, and 4) trace the redox processes in deep waters of the upper Chesapeake.

Quantitatively, this study uses mass balance calculations in order to model the mean scavenging residence times, defined by the mean dissolved ^{210}Po and ^{210}Pb adsorptive exchange rates onto particles. Such reaction sorption rates (λ_s) are defined as the scavenging rate constant for dissolved ^{210}Po and ^{210}Pb onto suspended particles and can be transposed to residence times. The results are compared between the two estuaries, as well as regionally for the Delaware estuary. These rates can be employed as proxies for other trace elements with similar biogeochemical behavior in order to determine their behavior and fate in the estuarine environment.

2 Material and Methods

Water samples for ^{210}Po and ^{210}Pb analysis were collected during April and August of 2012 for the Delaware and Chesapeake estuaries, respectively. The samples were collected aboard the R/V Sharp along the entire salinity gradient (0-31psu) in the Delaware and the upper Chesapeake estuaries (2-17psu) (Figure 1). At 34 stations surface (2m) and bottom samples at depth were collected using Niskin bottles, supplemented by the surface ship pump (SMS). Additional water samples were taken from intertidal waters of a lower Delaware salt marsh to investigate whether a salt marsh can act as a source or sink for ^{210}Po and ^{210}Pb radionuclides. This collection occurred over a 12-hour tidal cycle on 01 June 2012 at two sites, near the Roosevelt Inlet (RI) and within Canary Creek (CC) (Figure 1). A single end member sample was collected from Red Mill Pond, a primary freshwater source for the marsh (RMP, Figure 1).

A total of 34 Delaware estuary, 17 intertidal Delaware salt marsh, and 17 Chesapeake dissolved and particulate samples were collected. They were dispersed into 20L Cubitainers® filled with filtered seawater using Gelman Sciences sterilized Mini Capsule Filter membranes (<0.45 μm), and acidified to pH 2 using HCl. The cubitainers were sealed and stored in the dark until they were transferred into cold dark storage once ashore. The filtered and acidified seawater samples were assumed to be isolated from storage artifacts based on earlier findings (Chung and Craig, 1983). Separate subsamples were filtered through pre-weighed 0.45 μm polycarbonate membrane filters for ^{210}Po and ^{210}Pb particulates. Separate samples were collected on ashed glass fiber filters for POC and PON and placed in an -80°C freezer until processing. Polycarbonate membrane filters were subjected to HNO_3 digestion at 90°C for a day. Filtrate from POC and PON samples were collected and stored using HCl cleaned vials in order to analyze dissolved bay nutrients

228 (NO₃⁻, NH₄⁺, PO₄³⁻ and Si). Physiochemical parameters such as temperature, salinity,
dissolved oxygen, conductivity, fluorimetry, transmissometer were measured in-situ using a
230 CTD probes in the estuary and manual probes in the marsh (Seabird and YSI, Inc.).
Suspended particulate matter (SPM) was determined by weighed mass on the
232 polycarbonate filter.

Dissolved seawater samples were processed for ²¹⁰Po and ²¹⁰Pb using an established
234 protocol (Fleer and Bacon 1984) and modified according to Rigaud et al. (2013). Weighed
additions of ²⁰⁹Po isotope spike (1 dpm) and stable Pb carrier (20 mg) were added to each
236 sample for isotopic dilution analysis and chemical yield. The ²⁰⁹Po spike was calibrated
using two certified reference materials (IAEA-RGU-1 and NIST-SRM983) and found to be
238 2.12±0.05 dpm/g (35.3 ±0.8 mBq/g). Stable Pb carrier was calibrated using atomic
absorption. Nuclides were extracted by co-precipitation with Fe(OH)₃ (Thomson and
240 Turekian, 1976). The precipitate was recovered by filtration (0.45µm polycarbonate
Nucelpore) and then dissolved in a 0.5M HCl solution. In the case of particulate samples, the
242 solid phase is dried, weighed and spiked with ²⁰⁹Po and lead carrier before being completely
dissolved using a mixture of strong acids (including HF). The solution digest is evaporated
244 to near-dryness, any residue oxidized with nitric acid, reconstituted after several
evaporations in strong HCl, and recovered in 0.5M HCl solution. The ²¹⁰Po and ²⁰⁹Po were
246 plated in this solution by spontaneous deposition onto a silver disc heated in this solution
with about 200 mg of ascorbic acid (Flynn, 1968) and their activities measured by alpha
248 spectroscopy. A small aliquot of the solution was taken from this solution in order to
measure Pb recovery from the time of collection. The remaining Po in solution was
250 removed in 9 M HCl using AG-1X8 anion exchange resin as described by Sarin et al., (1992).
After separation, another small aliquot was taken from the final eluate solution containing
252 the ²¹⁰Pb to gauge the Pb yield during subsequent in-growth of ²¹⁰Po from ²¹⁰Pb and both
measured using Flame atomic absorption to determine Pb recovery. The final eluate
254 solution was re-spiked with ²⁰⁹Po and stored at least 6 months to allow in-growth of ²¹⁰Po
from ²¹⁰Pb. The ²¹⁰Pb activity of the samples was then determined by plating the eluate
256 solution on another silver disc, via the in-growth of ²¹⁰Po.

Finally, the determination of the initial activities of ²¹⁰Po and ²¹⁰Pb at the time of collection
258 was calculated using the equations and corrections accounting for decay and ingrowth of
the nuclides, which are detailed in Rigaud et al., (2013). High errors on a few ratios are due
260 to low activity concentrations, as is normal when sample volumes are limited. Overall,

errors were <10% for most samples. Duplicate blanks were determined by processing a liter of distilled water in the same way as the samples to correct the calculated activities (<4% sample activity). Detector background was individually subtracted from each sample activity (<3%). The reproducibility of the method was tested based on duplicate analysis of five different stations with the relative variations found to be 3.3% between duplicate analyses.

268 3. Results

The radionuclide activities and associated errors are presented in Table 1 for the Delaware and Chesapeake estuaries and in Table 2 for the Delaware salt marsh. Two dimensional distribution plots of ^{210}Po , ^{210}Pb , and $^{210}\text{Po}/^{210}\text{Pb}$ activity ratios in the dissolved and particulate phases for the Chesapeake and Delaware estuaries were created using Ocean Data View (ODV)(Schlitzer, 2013) (Figures 2 and 4). All of the physiochemical data, which includes temperature, salinity, dissolved oxygen, conductivity, suspended matter and chemical analysis of POC, PON, NO_3^- , NH_4^+ , PO_4^{3-} and Si, are reported in the Supplemental Materials (including Figures 2 and 4 in color).

278 3.1 Delaware Estuary

Throughout the Delaware estuary, the salinity and temperature display well mixed features from the surface to within a few meters of the bottom. Increased temperatures were observed in the upper estuary and gradually decreased towards the high salinity coastal waters. Dissolved oxygen (DO) concentrations were constant (93% DO saturation) in the upper estuary, increased to 96% in the surface waters of the mid estuary, and ultimately decreased to concentrations of <90% in the lower estuary. The maximum oxygen and fluorometer signal, along with a decrease in dissolved nutrient concentrations of NO_3^- , NH_4^+ , PO_4^{3-} , are indicative of a phytoplankton bloom in the mid to lower estuary. This occurrence is common in the Delaware estuary, as reported by Voynova and Sharp (2012). The upper estuary exhibits low concentrations of suspended particulate matter (3.91mg/L) that dramatically increase to 35 mg/l in the mid estuary, where a turbidity maximum is found.

Dissolved ^{210}Po concentrations in the Delaware estuary ranged from 1.3 dpm/100L in the upper estuary to 4.7 dpm/100L in the lower estuary (Table 1 and Figure 2). Dissolved ^{210}Pb concentrations varied from 1.0 to 4.0 dpm/100L, with the greatest variation occurring

294 in the lower estuary deep waters (0.91 dpm/100L) and in the mid estuary where the
phytoplankton bloom occurred. The dissolved $^{210}\text{Po}/^{210}\text{Pb}$ activity ratios in the upper
296 estuary (0-50km transect distance) were less than one, while an excess (>1) was present in
the mid to lower estuary.

298 Particulate concentrations of ^{210}Po and ^{210}Pb ranged from 1.1 to 18 and 0.42 to 60
dpm/100L, respectively. Particulate ^{210}Po concentrations were highest in the turbidity
300 maximum, defined by the transmissometer readings and weighed filters of particulate
matter. The particulate ^{210}Pb maximum was located in the intermediate waters of the upper
302 estuary, while the minimum was found at the surface and bottom samples throughout the
lower estuary. Of the total concentration in ^{210}Po , 60% was found in the dissolved phase at
304 the headwaters (sample DB01) and decreased within the turbidity maximum to 11% before
increasing again in the lower bay to 68%. Of the total concentration, dissolved ^{210}Pb activity
306 comprised 12% in the headwaters and dropped to 3% in the turbidity maximum.

308 *3.2 Lower Delaware Salt Marsh (Canary Creek)*

Intertidal sampling occurred at two locations, Roosevelt Inlet (entrance) and Canary
310 Creek (upstream). The salinity concentrations over the tidal cycle ranged between 27-29
and 20-24 psu for the Roosevelt Inlet and Canary Creek sampling sites, respectively
312 (Supplemental Materials). Here is noted that little difference between the temperature,
dissolved oxygen, and NO_3^- concentrations for each sampling site and over the tidal cycle.
314 POC, PON, Si and PO_4^{3-} concentrations were greatest at high tide in Canary Creek, while
Roosevelt Inlet concentrations were constant over the tidal cycle (Supplemental Materials).

316 Dissolved ^{210}Po ranged from 2.8 to 9.9 dpm/100L at Roosevelt Inlet and 3.9 to 14
dpm/100L at Canary Creek (Table 2 and Figure 3). In the sample collected at Red Mill Pond,
318 the fresh water end member of the creek, ^{210}Po activity was 9.0 dpm/100L. Over the tidal
cycle, ^{210}Po activities in Canary Creek increased during the flooding tide, while activities
320 increased during low tide at Roosevelt Inlet. Dissolved ^{210}Pb ranged from 1.2 to 12
dpm/100L at Roosevelt Inlet and from 4.6 to 14 dpm/100L at Canary Creek, while it was
322 higher (19 dpm/100L) at Red Mill Pond (Table 2). The maximum dissolved ^{210}Po and ^{210}Pb
for Roosevelt Inlet were both observed during low tide. Interestingly, at Canary Creek,
324 farthest from tidal influence, ^{210}Po reached a maximum at flooding tide and ^{210}Pb at ebbing
tide. Dissolved $^{210}\text{Po}/^{210}\text{Pb}$ activity ratios at Canary Creek indicated a similar to greater
326 proportion of ^{210}Pb versus ^{210}Po (≤ 1) during high, ebbing and low tide, while a dissolved

328 ^{210}Po excess (>1) was measured during flooding tide (up to 2.3 ± 0.3). In Roosevelt Inlet,
330 $^{210}\text{Po}/^{210}\text{Pb}$ ratio presented the opposite trend, with significant excess at high to ebbing tide
and values close to equilibrium during and following low and flooding tide.

332 *3.3. Upper Chesapeake Estuary*

332 During late summer, the upper Chesapeake estuary can be divided into two main
zones: an upper zone (from 0-10m) that is vertically well mixed along the upper extent (0-
334 50km), and with deeper waters (10-25m) isolated by a strongly stratified water column
along a lower zone (60-120km) according to temperature and salinity (Supplemental
336 Materials). In the vertically well-mixed upper zone, salinity ranged from 3 to 10 psu with a
constant temperature of 27°C . In the upper well-mixed zone of the estuary, a turbidity
338 maximum was present with suspended particulate matter concentrations greater than
60mg/L (Supplemental Materials). These high suspended sediment concentrations were
340 constant until midway down the estuary and decreased to <10 mg/L in the lower estuary.
Dissolved nutrient concentrations of NO_3^- and Si at the mouth of the Susquehanna River
342 reached a maximum and decreased down the estuary, while the opposite trend was
observed for NH_4^+ and PO_4^{3-} . In the upper stratified zone the water column exhibited well-
344 oxygenated surface water (90% DO above 12 m depth) and suboxic/anoxic ($\text{O}_2 < 1\%$ DO)
bottom waters below (Supplemental Material).

346 Dissolved radionuclide concentrations along the upper Chesapeake ranged from 0.8 -
4.4 dpm/100L and 0.4 - 4.3 dpm/100L for ^{210}Po and ^{210}Pb , respectively (Table 1 and Figure
348 4). The first sample near the headwaters of the Chesapeake estuary consisted of high
dissolved ^{210}Po concentrations (4 dpm/100L). These concentrations decreased to 1-
350 2.5dpm/100L seaward (to 40 km), with a mid-depth water column increase to 5 dpm/100L
at 120km (Figure 4). The dissolved ^{210}Pb activity was generally constant at 1 dpm/100L
352 throughout the upper Chesapeake estuary, except for two samples: 60km (at surface) and
120km (at depth) transect distance (2-5 and 3-5 dom/100L, respectively). At 60km transect
354 distance, an enrichment of 4.0 dpm/100L of dissolved ^{210}Pb was observed in the vicinity of
the Baltimore Harbor. North of the Potomac, a suboxic zone was associated with increases
356 in dissolved ^{210}Pb and ^{210}Po concentrations. Here between 7m and 12m the dissolved ^{210}Po
(4.4 dpm/100L) and ^{210}Pb (3.0 dpm/100L) concentrations were at a maximum before
358 decreasing to 1 dpm/100L in lower oxygenated waters (below 12m). An excess of dissolved

360 $^{210}\text{Po}/^{210}\text{Pb}$ activity ratio (>1) was observed over most of the Chesapeake estuary, and at depth two locations (55km and 120km) reached a ratio of 5 (Table 1 and Figure 4).

362 Particulate concentrations ranged from 0.3 to 31 dpm/100L and from 0.3 to 67 dpm/100L for ^{210}Po and ^{210}Pb , respectively. In the upper estuary, the radionuclide particulate concentrations were associated with similar trends to the suspended matter at 364 the turbidity maximum (0-20 km), as noted by Chuch and Sarin, 1995. The highest particulate activity for ^{210}Pb was located (120km transect distance) at 15m in the sub-oxic 366 bottom waters (67 dpm/100L), while the highest particulate activity for ^{210}Po (31 dpm/100L) was located at 10m depth (15km). The proportion of total ^{210}Po in the dissolved 368 phase at the freshwater end member (CB01) was 6% and increased gradually to 26% until 60km transect distance. ^{210}Pb increased from 3% to 28% until 60km transect distance. At 370 this point the percent of ^{210}Po in the dissolved phase changed to 83% while, the ^{210}Pb increased to 58%.

372

4 Discussion

374 The ^{210}Po and ^{210}Pb dynamics will be discussed in association with the main characteristics observed in both estuaries. These characteristics include, the turbidity 376 maximum, phytoplankton blooms, exchanges with surrounding salt marshes along the Delaware estuary, and redox chemistry at the oxic/anoxic transition in the Chesapeake 378 estuary. Finally, box-model calculations for both estuaries will be applied to determine dissolved-particulate sorption rates that translate to scavenging residence times.

380

4.1 ^{210}Po and ^{210}Pb cycling in the maximum turbidity zone

382 Maximum turbidity zones were found in both the upper Delaware and Chesapeake estuaries and corresponded to a decrease of dissolved nuclides and an increase of 384 particulate nuclide activities. This is clearly illustrated when reporting the differential removal of dissolved versus total nuclides. Indeed, outside the turbidity maximum zone, 386 ^{210}Po is mainly present under dissolved form $59 \pm 6\%$ in the Delaware and $55 \pm 5\%$ in the Chesapeake. However this proportion decreased to $11 \pm 1\%$ and $7 \pm 1\%$ in the turbidity zone 388 for the Delaware and the Chesapeake, respectively. Similarly, ^{210}Pb is mainly present in the dissolved form $66 \pm 5\%$ in the Delaware and $51 \pm 5\%$ in the Chesapeake outside of the 390 turbidity zone. Within the turbidity zone, the proportion decreases to $3 \pm 1\%$ in the Delaware and $3 \pm 1\%$ in the Chesapeake.

392 Such observations suggest that ^{210}Po and ^{210}Pb undergo marked chemical transfers
from the dissolved to the particulate phases in the turbidity zone, as ^{210}Pb has a strong
394 surface particle affinity (Benninger, 1978). It is suggested that ^{210}Pb transfer from the
dissolved to particulate phase is due to surface adsorption of ^{210}Pb onto surface particles.
396 This is further enhanced in the turbidity zone due to the increase of the available surface
particulate sorption sites. However, in the case of ^{210}Po , adsorption process and biological
398 uptake may both be involved in ^{210}Po transfer, although this is unlikely in the turbidity
maximum zone.

400 These observations in two distinct estuarine systems give evidence that most ^{210}Po
enters estuaries in the dissolved phase. However, most ^{210}Pb enters the estuaries in the
402 particulate phase or is scavenged further upriver in each system. Within the turbidity
maximum, both nuclides are rapidly scavenged as previously reported in estuarine systems
404 (Church and Sarin, 1986; Benninger, 1978). Both studies reported that ^{210}Pb and ^{210}Po
become largely associated with suspended particles and tightly correlated in the low
406 salinity turbidity maximum. This is in agreement with our findings of nuclide scavenging
within the turbidity maximum for both the Delaware and Chesapeake estuaries. The
408 increased ^{210}Po and ^{210}Pb activity ratios in the particulate phase ($\text{Po}/\text{Pb} > 1$) indicating
higher scavenging of ^{210}Po , most likely the result of bioaccumulation.

410

4.2 ^{210}Po and ^{210}Pb cycling with phytoplankton bloom

412 In each estuary, a phytoplankton bloom was present and led to scavenging and
subsequent remineralization of nuclides. Within the entire Delaware water column a bloom
414 was observed (75-90km). Correspondingly in the Chesapeake surface waters (0-5m) the
bloom was evident from 50-120km. This was indicated by a higher fluorimetry signal
416 coupled with corresponding nutrient data (Supplemental Materials). In these areas the
 ^{210}Po and ^{210}Pb activity ratios in the particulate ($\text{Po}/\text{Pb} > 1$) indicates higher scavenging of
418 ^{210}Po from the possibility that bioaccumulation may have occurred. The Delaware bloom
displays these conditions with a particulate Po/Pb ratio that ranged from 4 to 6, while
420 within the Chesapeake bloom a ratio of 2.5-3 is observed (Figure 2 and 4). Another
illustration to support the observation of bioaccumulation is the dissolved nuclides versus
422 particulate nuclides. The proportion of total dissolved ^{210}Po in the surface water at the point
of the proposed bloom was $17 \pm 3\%$ in the Delaware and $38 \pm 4\%$ in the Chesapeake. Notably
424 greater was, the proportion of total dissolved ^{210}Pb within the bloom area in the Delaware

at 50% and 46% in the Chesapeake. This suggests that biogeochemical processes in the
426 bloom act as efficiently to either solubilize both nuclides or allow greater particulate
removal.

428 Remineralization of nuclides down estuary within the bloom (Delaware) and at depth
within the water column (Chesapeake) also leads to increased distribution of dissolved
430 versus particulate ^{210}Po activities. In these areas estuarine conditions resulted in the
dissolved ratio $^{210}\text{Po}/^{210}\text{Pb}$ to range from 2-2.5 and 3.5-5 for the Delaware and Chesapeake,
432 respectively (Figure 2 and 4). Here too the proportion of dissolved versus particulate
nuclide for dissolved ^{210}Po was 68% in the whole Delaware and 73% in the Chesapeake.
434 Such differential behavior implies that the ^{210}Po has been regenerated in the mid-salinity
surface water region (100-150km) within the Delaware and at depth within the
436 Chesapeake. It is important to note that this trend does not continue at deeper depths
($>10\text{m}$), as the waters become suboxic.

438 Previous studies within the Delaware estuary (Church and Sarin, 1995) included only
surface samples and thus were not able to observe the regeneration processes occurring at
440 bottom depths during times of high productivity in the Delaware estuary. Thus it is
proposed that the scavenging and regeneration of ^{210}Po and ^{210}Pb occurs in a similar
442 manner to that at depth in the open ocean. In the open ocean there is a preferential transfer
of ^{210}Po from the dissolved phase to the particulate phase by bioaccumulation in surface
444 waters and export to the subsurface by the settling of particles (i.e., scavenging) (Stewart, et
al., 2007). In a vertically stratified trench, this sorption step appears to be very fast (hours)
446 and becomes evident during times of high productivity, such as during spring and summer
months. In deeper ocean waters, the remineralization of particulate matter results in a
448 release of ^{210}Po from the particles to the dissolved phase (Bacon et al., 1976, 1978; Cochran
et al., 1983; Stewart and Fisher, 2003a; Stewart et al., 2007). It appears that these processes
450 can occur on time scales comparable to larger estuaries as documented in this study.

452 *4.3 ^{210}Po and ^{210}Pb cycling in salt marshes (and exchange with the Delaware estuary)*

The dissolved concentrations for both radionuclides in the Delaware intertidal marsh
454 are generally higher than those measured in the estuary and coastal waters (Table 2). The
radionuclides also present strong variations over tidal cycles and furthermore differ
456 between the two sampling sites, located at the entrance of the salt marsh (Roosevelt Inlet;
RI) and within the salt march (Canary Creek; CC) (Figure 3). These variations, which

458 transpire over a 12hr tidal cycle, are a result of rather rapid biogeochemical and physical
processes occurring within the salt march.

460 At RI, both dissolved radionuclides follow the same trend throughout the tidal cycle
with a maximum activity (10 dpm/100L) present at low tide. During low tide, the dissolved
462 proportion of the water from the salt march at RI is greatest. The high activity values also
found at low tide suggest the salt marsh as a source for both ^{210}Po and ^{210}Pb to Delaware
464 Bay. At low tide, the activity ratio is about 1, which indicates similar and older sources of
 ^{210}Po and ^{210}Pb . Conversely, an activity ratio of >1 is present during high and ebbing tide,
466 which evidence a greater proportion of water from the Delaware estuary.

On the other hand, the interior (CC) concentration of dissolved ^{210}Po reached a
468 maximum (14 dpm/100L) at flooding tide, while the dissolved concentration of ^{210}Pb
reached a maximum (14 dpm/100L) during ebbing tide. At flooding tide, ^{210}Po activity at CC
470 is notably higher than in the Delaware Bay and RI. In addition, the increase in activity ratio
of $^{210}\text{Po}/^{210}\text{Pb} >1$ during the flooding tidal transit from RI to CC indicates remineralization of
472 ^{210}Po -bearing particles, which originated in the Delaware Bay. During high tide in CC, the
 ^{210}Po decreased and reached equilibrium with ^{210}Pb , which indicates that the ^{210}Po is
474 released then scavenged within the marsh at high tide. Contrarily, the maximum dissolved
 ^{210}Pb activity during ebbing tide may be caused by ^{210}Pb inputs within the marsh, such as
476 redox mobilization during groundwater discharge. This input is then conserved during the
ebbing tidal transit from CC to RI when a ^{210}Pb maximum occurred at low tide, supporting a
478 continuous groundwater discharge.

The difference in nuclide behavior between salt marsh sites indicates that the
480 dissolved ^{210}Po from the Delaware Bay entering the marsh is removed during flooding tide.
The ^{210}Po removal processes within the marsh could also be associated with the ^{210}Po
482 bioaccumulation by vegetation (Church, 1986), and ^{210}Pb scavenging by sedimentation with
other proxy trace elements such as stable Pb (Kim, et al. 2004). Alternatively, dissolved
484 ^{210}Po could be precipitated by the marsh sediments during the reduction of sulfur, its
elemental analogue (Luther and Church, 1988). In any case, the data suggests that the salt
486 marsh is a probable net source of dissolved ^{210}Pb to the surrounding estuary. Such
processes would support our findings of higher levels of dissolved ^{210}Pb and ^{210}Po are found
488 within the marsh compared to the surrounding estuary.

490 *4.4 ^{210}Po and ^{210}Pb cycling at oxic/suboxic interface*

492 In order to investigate processes in an estuarine redox environment, ^{210}Po and ^{210}Pb
nuclides can be an important tool. The upper Chesapeake Bay contains a pervasive suboxic
and anoxic deeper zone, which occurs at depths as shallow as 5 to 10m. However, during
494 the August 2012 cruise only sub-oxic waters were evident below 12m in the mid-estuary
(75-120km) (Supplemental Materials). In surface waters (0-10m) from 100-125km, an
496 elevated $^{210}\text{Po}/^{210}\text{Pb}$ activity ratio in the particulate phase of 4 indicates preferential
scavenging of ^{210}Po from bioaccumulation (Figure 4). The proportion of total particulate
498 ^{210}Po in the surface water was $68\pm 5\%$. As the waters approach suboxic levels, a pycnocline
(10m) arises and can be identified by high dissolved ^{210}Po and ^{210}Pb activity, 5 and 4
500 dpm/100L, respectively (Table 1). The proportion of total dissolved ^{210}Po and ^{210}Pb
increased at the pycnocline to $86\pm 5\%$ and $63\pm 4\%$, respectively; indicating that regeneration
502 of the nuclides has taken place. Interestingly, below the pycnocline (12-20m) the activity of
both radionuclides in the particulate phase largely increased, 10 dpm/100L in ^{210}Po and 80
504 dpm/100L in ^{210}Pb . As such, the proportion of nuclides in the particulate phase increased to
 $80\pm 7\%$ and $98\pm 6\%$ for ^{210}Po and ^{210}Pb , respectively.

506 We hypothesize that the solubilized ^{210}Po and ^{210}Pb seen at 12m depth is due to sub-
oxic reduction and dissolution of MnO_2 . The newly released dissolved ^{210}Po and ^{210}Pb diffuse
508 upward in the water column towards the sub-oxic boundary for scavenging by MnO_2 .
Alternatively, the nuclides could diffuse downward towards anoxic sediments where ^{210}Pb
510 and ^{210}Po could be permanently removed from the water column by sulfide co-precipitation.
Thus, we propose that in the upper Chesapeake Bay, the water column profiles of ^{210}Po and
512 ^{210}Pb in sub-oxic areas are influenced by the redox cycling of Fe/Mn oxides at the water
column pycnocline, or Fe sulfides at depth. This is analogous to the vertically stratified
514 anoxic oceanic systems as follows.

There are limited investigations of the aqueous geochemistry of ^{210}Po and ^{210}Pb at
516 sub-oxic and anoxic interfaces in the open ocean (Bacon et al., 1980; Todd et al., 1986; Wei
and Murray, 1994), and none exist for an estuarine environment. From these few studies we
518 know the following; at the pycnocline particulate ^{210}Po and ^{210}Pb show evidence of
enrichment relative to mid-depth water column values (Todd, et al., 1986). In the region
520 above the redox interface where MnO_2 begins aerobic reduction and dissolution, MnO_2 -
bound ^{210}Po and ^{210}Pb becomes solubilized (Bacon et al., 1980; Wei and Murray, 1994). In
522 contrast, FeOOH-bound ^{210}Po and ^{210}Pb are not released here because Fe does not undergo
reduction and dissolution until the anoxia is reached.

524 Observations from the Chesapeake estuary data agree with the oceanic studies and
526 suggest similar behavior of ^{210}Po and ^{210}Pb across the oxic/anoxic interface in an estuarine
528 environment. Previous studies of the Chesapeake Bay characterized the chemical structure
530 of the water column during periods of anoxia (Luther et al., 1994). Prominent features
532 include the presence of a redox front, defined by the $\text{O}_2/\text{H}_2\text{S}$ interface, and the presence of a
534 well defined manganese-rich particulate layer above the interface. In this region particulate
536 Fe (III) and Mn (III, IV) are reduced to their divalent states, thus solubilized with reduced
electron activity (Luther et al., 1994). As the dominant carrier phase of many metals and
radionuclides, Fe and Mn oxide dissolution and precipitation at the $\text{O}_2/\text{H}_2\text{S}$ interface can
determine the fate of such particle reactive elements. Furthermore, redox reaction involving
sulfur species in anoxic waters can form aqueous polysulfide ions to efficiently scavenge
many free metals, such as Pb^{+2} , to form highly insoluble phases such as galena, PbS (Stumm
and Morgan, 1981; Luther and Church, 1988).

538 *4.5 Residence times*

Under different conditions within both estuaries (phytoplankton bloom, max turbidity
540 zone, anoxic/oxic interface) both ^{210}Po and ^{210}Pb are primarily scavenged on particles,
inducing disequilibrium, which is used to estimate the net scavenging residence time. A
542 scavenging rate constant for transfer of dissolved ^{210}Po and ^{210}Pb onto suspended matter is
based on a simple box model (Figure 5). This rate can then be translated into scavenging
544 residence times. The Delaware Bay geomorphology matches that of a typical estuary with a
broad inner bay bound by two cape entrances, with partially mixed characteristics. As such
546 the Delaware Bay meets the general requirements of a simple box-model based on a mass
balance of the radionuclides between phases. From this we assume that measured
548 concentrations of radionuclides (Table 1) are representative of yearly spring and summer
annual periods. The estuaries may be characterized by a single (upper Chesapeake estuary)
550 or three successive (upper, mid, and lower Delaware estuary) box-models, each assuming
steady-state conditions are maintained for several months (Figure 5).

552 The balance of dissolved ^{210}Po concentrations in the estuary depends upon the
following: discharges of dissolved ^{210}Po into the estuary, ^{210}Po produced through
554 radioactive decay of dissolved ^{210}Pb , ^{210}Po removal from solution, and ^{210}Po exported with
the water discharged to the coastal sea. Therefore, the mass balance equation for dissolved
556 ^{210}Po in the estuary is

$$\lambda_{Po}A_{Pb} + I_r + I_{smPo} + \lambda_{Po}I_{smPb} + I_{aPo} + \lambda_{Po}I_{aPb} = \lambda_{Po}A_{Po} + \lambda_sA_{Po} + \lambda_wA_{Po} \quad (1)$$

558 All parameters and rates as noted are specified in Figure 5 and Table 3. Substituting
the data into the equation (1) and solving for λ_s , the scavenging rate constant in the
560 Delaware estuary for ^{210}Po onto suspended matter and sediment particles, is 4.2 a^{-1} . A
corresponding residence time of ^{210}Po can be translated for the whole estuary as 86 days.
562 The ^{210}Po is exported at a rate that is consistent with about 60% of the annual delivery of
dissolved ^{210}Po into the estuary. Therefore, only 40% of the dissolved ^{210}Po , entering or
564 generated in the estuary from the decay of ^{210}Pb , is removed by sorption onto sedimentary
particles and trapped in the estuary and intertidal marshes.

566 In the Delaware estuary sufficient data allows an upper, mid, and lower region to be
readily defined (on the basis of salinity) into three box-models zonally distributed to
568 distinguish successive estuarine processes. Similarly, the same equations can be abridged
using values for each specific region of the Delaware. Using the concentration of dissolved
570 ^{210}Po broken down by region (i.e. upper, mid, and lower) results in scavenging residence
times of 22 days, 20 days, and 25 days, with errors of less than one day per region. Though
572 the residence times do not display a large range between regions, they differentiate
between different scavenging processes: onto suspended particles (turbidity maximum,
574 upper estuary), biogenic scavenging during phytoplankton blooms (mid estuary), and a
combination of regeneration and salt marsh exchange (lower estuary).

576 An identical mass balance equation may be written for dissolved ^{210}Pb in the Delaware
with:

$$\lambda_{Pb}A_{Ra} + I_r + I_{smPb} + \lambda_{Pb}I_{sm} + I_a + \lambda_{Pb} = \lambda_{Pb}A_{Pb} + \lambda_sA_{Pb} + \lambda_wA_{Pb} \quad (2)$$

578 where, λ_{Pb} is the radioactive decay constant ^{210}Pb , $\lambda_{Pb}A_{Ra}$ corresponds to the ^{210}Pb
580 ingrowth from dissolved ^{226}Ra in the estuary and the other variables similar to those
already introduced (Figure 5 and Table 3). The contribution of ^{226}Ra from atmospheric
582 deposition is assumed to be negligible. The input of dissolved ^{226}Ra through radioactive
decay as a source of total dissolved ^{210}Pb also is also assumed to be minimal, compared with
584 other ^{210}Pb sources primarily weathering of particles in the watershed or atmospheric
deposition.

586 Solving equation (2), λ_s , defined as the scavenging rate constant for dissolved ^{210}Pb
onto suspended sediment particles, is 5.5 a^{-1} , and as transposed inversely, a mean residence
588 time of soluble ^{210}Pb in the whole Delaware estuary of 67 days. This discharge of soluble
 ^{210}Pb to coastal waters accounts for 55% of the annual input received by the estuary, which

590 includes atmospheric deposition. Therefore, most of the ^{210}Pb entering the estuary in the
soluble phase is either absorbed onto suspended particles and trapped in sediment
592 accumulation zones of the estuary, such as intertidal marshes, or discharged via binding to
suspended matter into the coastal ocean. As with ^{210}Po , the ^{210}Pb residence time for the
594 Delaware estuary can be differentiated by zonal region resulting in times of 21 days
(upper), 14 days (mid), and 10 days (lower) that notably decrease down estuary.

596 Utilizing a similar approach, mean residence times for surface waters of the upper
portions of the Chesapeake estuary in the summer were calculated using a single box-
598 model. As the sampling focused only on the upper Chesapeake, a zonal approach was not
applied. The upper estuary of the Chesapeake is defined here as the oxic region extending
600 from the mouth of the Susquehanna River, seaward to the mouth of the Potomac Estuary
and from 0-5 meters in depth. This region encompassing the upper bay includes the eastern
602 and western tributaries, which include 1484 km² and 14% of the total Chesapeake Bay area
(Ranasinghe et al., 1998). Unlike the Delaware estuary, there are essentially no significant
604 intertidal marshes surrounding the upper bay, thus no marsh exchange is considered. Using
the data from Table 1, the scavenging rate constant for dissolved ^{210}Po onto suspended
606 matter and sediment particles is 2.91a^{-1} . The mean residence time of ^{210}Po in solution
relative to adsorption on sediment particles is translated to be 125 days, while dissolved
608 ^{210}Pb scavenging rate is 6.6a^{-1} , with the mean residence time translated as 55 days.

Comparing the two single-box model residence time results of ^{210}Po for the entire
610 estuary, Delaware (87 days) and the Chesapeake (126 days), suggest that biogenic cycling is
greater in the upper Chesapeake estuary. However, ^{210}Pb scavenging residence times of the
612 Delaware (66 days) and the Chesapeake (53 days) suggest that the physicochemical
adsorption on particles is slightly greater in the Delaware. It is hypothesized that other
614 trace elements with similar chemical characteristics as ^{210}Pb (Type A) and ^{210}Po (Type B)
will present similar sorption rates. "Type A" trace metals tend to form cations, which react
616 with negatively charged ions and suspended particles, including elements such as Fe, Mn, Co
and Cr (Church, 1986). However, "Type B" metals tend to form stronger complexes with
618 organic matter, which include elements such as Zn, Ni, Cu, Cd, Ag, and Hg.

620 **5.1 Conclusions**

The following conclusions and implications of geochemical cycling of ^{210}Po and ^{210}Pb
622 in the estuarine waters of the Delaware and Chesapeake Bays can be made. Both upper

624 estuaries are influenced by maximum turbidity zones, which correspond to a decrease in
dissolved and an increase of particulate nuclide activities. Outside the turbidity maximum
626 zone, ^{210}Po is mainly present in the dissolved form at $59 \pm 6\%$ in the Delaware and $55 \pm 5\%$
in the Chesapeake, while this proportion decreased to $11 \pm 1\%$ and $7 \pm 1\%$ in the turbidity
zone for the Delaware and the Chesapeake, respectively.

628 Phytoplankton blooms in both estuaries scavenge ^{210}Po in surface waters and are
regenerated at depth similar to processes seen in the open ocean. The scavenging by
630 biological particles is one of the main processes that affect nuclide distribution found in
lower sections of the estuaries. Regeneration occurs at depth for more stratified systems in
632 the Chesapeake and further down the estuary in the Delaware. In a lower Delaware salt
marsh sources of ^{210}Pb and ^{210}Po are evident during tidal cycling. Within the Delaware salt
634 marsh scavenging and regeneration of ^{210}Po occurs, whereby ^{210}Po is released by biological
particles during low tide and scavenged during high tide. In the Chesapeake estuary redox
636 chemistry at the oxic/suboxic transition show a release of radionuclides at the pycnocline
and scavenging as the waters become more anoxic, proposed evidence of redox cycling from
638 Fe/Mn oxides. In the Delaware, box-model calculations result in ^{210}Po residence times for
three successive regions similar at 20-25 days, while ^{210}Pb decreased from 20 to 10 days
640 from the upper to lower estuary. The upper Chesapeake has a longer residence time, 125
days for ^{210}Po and 55 days for ^{210}Pb due to greater biological scavenging and stratified
642 waters than the Delaware. The use of the radionuclides ^{210}Po and ^{210}Pb to determine
residence times can also be applied as proxies for other Type A (^{210}Po) or Type B (^{210}Pb)
644 trace elements and thus potential pollutant impacts such elements have on estuarine
systems.

646

648

650

652

654

656

658

660

Acknowledgements

662 -Dr. Luther for providing research cruise time in the Delaware and Chesapeake supported
by NSF/OCE grants 1031272 and 1059892.

664 -Graduate support for D. Marsan was provided by NSF Grant- HRD-1139870- Greater
Philadelphia Region LSAMP Bridge to the Doctorate (Cohort IX)

666 -Post-Doctoral support for S. Rigaud was provided by NSF/OCE grant 0961653.

668

670

672

674

676

678

680

682

684

686

688

690

692

694

696

698

700

702

704

706

REFERENCES

- 708 Bacon, MP., Spencer, D.W., Brewer, P.G. 1976. $^{210}\text{Pb}/^{226}\text{Ra}$ and $^{210}\text{Po}/^{210}\text{Pb}$ disequilibria
710 in seawater and suspended particulate matter. *Earth Planet. Sci. Lett* 32, 277-296.
- 712 Bacon, M.P., Brewer, P.G., Spencer, D.W., Murrery, J.W., 1980. Lead-210, polonium-210
714 manganese and iron in the Cariaco Trench. *Deep Sea Res.* 27, 119-135.
- 716 Benninger, L.K.,(1978) ^{210}Pb balance in Long Island Sound. *Geochimica et Cosmochimica*
Acta 42 (8), 1165-1174.
- 718 Carvalho, F., 1997. Distribution, cycling and mean residence time of ^{226}Ra , ^{210}Pb and
720 ^{210}Po in the Tagus estuary. *The Science of the Total Environment* 196, 151-161.
- 722 Chung, Y., Chang, W.C., 1995. Pb-210 fluxes and sedimentation rates on the lower
continental slope between Taiwan and south Okinawa Trough. *Continental Shelf Research*
15, 149-164.
- 724 Chung, Y., and Craig, H. 1983. ^{210}Pb in the Pacific: the GEOSECS measurements of
particulate and dissolved concentrations. *Earth and Planetary Sci.*, 65 406-432.
- 726 Church, T.M., 1986. Biogeochemical factors influencing the residence time of
microconstituents in a large tidal estuary, Delaware Bay. *Mar. Chem.* 18, 393-406.
- 728 Church, T.M., M. Bernat & P. Sharma, 1987. Distribution of natural uranium, thorium, lead
730 and polonium radionuclides in tidal phases of a Delaware salt marsh. *Estuaries* 9: 2-8.
- Church, T., Sarin, M.. 1995. Natural U-Th series radionuclide studies of estuarine
732 processes, in: Dyer, K.R., Orth, R.J. (Eds.), *Changes in Fluxes in Estuaries: Implication From*
Science to Management. Proceedings of the ECSA22/ERF Symposium, Plymouth, England,
734 *September 13-18,1992, pp.91-95.*
- 736 Cochran, JK., Masqué,, P.,. 2003. Short-lived U/Th Series Radionuclides in the Ocean: Tracers
for Scavenging Rates, Export Fluxes and Particle Dynamics. *Reviews in Mineralogy and*
738 *Geochemistry* 52, 461-492.
- 740 Fleer, A.P., Bacon, M.P., 1984. Determination of ^{210}Pb and ^{210}Po in seawater and marine
particulate matter. *Nuclear Instruments and Methods in Physics Research* 223, 243-249.
- 742 Flynn, W. W., 1968. The determination of low levels of polonium-210 in environmental
744 materials. *Anal. Chim. Acta* 43, 221-227.
- 746 Heussner, S., Cherry, R.D., Heyraud, M., 1990. ^{210}Po , ^{210}Pb in sediment trap particles on a
Mediterranean continental margin. *Continental Shelf Research* 10, 989-1004.
- 748 Kim, G., Hussain, N. Church, T., 2000. Excess ^{210}Po in the coastal atmosphere. *Tellus.* 52B,
750 74-80.

- 752 Kim, G., Alleman, L.Y. , and T.M Church. 2004. Accumulation records of radionuclides
and trace metals in two contrasting Delaware salt marshes." *Marine Chemistry*, 87: 87-
96.
- 754
- 756 Kim, G., Kim, S., Harada, K., Schultz, M., Burnett, W. 2005. Enrichment of Excess ^{210}Po in
Anoxic Ponds. *Environ. Sci. Technol.* 39, 4894-4899.
- 758 Luther, G.W. III, Church, T.M., 1988. Seasonal cycling of sulfur and iron in porewaters of a
Delaware salt marsh. *Mar. Chem.* 23, 295-310.
- 760
- 762 Luther, G.W. III, Church, T.M., 1988. Seasonal cycling of sulfur and iron in porewaters of a
Delaware salt marsh. *Mar. Chem.* 23, 295–310.
- 764 Luther, G.W. III, Nuzzio, D.B., Wu, J., 1994. Speciation of manganese in Chesapeake Bay
waters by volumetric methods. *Anal. Chim. Acta* 284, 473-480.
- 766 McKee, B.A., Todd, J.F., 1993. Uranium behavior in a permanently anoxic fjord: microbial
control? *Limnol. Oceanogr.* 38, 408-414.
- 768
- 770 Millward, G.E., Turner, A., 1995. Trace elements in estuaries. In: Salbu, B., Steinnes, E. (Eds.),
Trace Metals in Natural Waters. CRC Press, Boca Raton, FL, pp. 223–245.
- 772 Nozaki, Y., 1986. ^{226}Ra - ^{222}Rn - ^{210}Pb systematics in seawater near the bottom of the
ocean. *Earth and Planetary Science Letters* 80, 36-40.
- 774 Nozaki, Y., J. Thomson, and K. K. Turekian. 1976. The distribution of ^{210}Pb and ^{210}Po in the
surface waters of the Pacific Ocean. *Earth Planet. Sci. Lett* 32, 304-312.
- 776
- 778 Ranasinghe, J.A., Scott, L.C. Kelly, F.S., 1998. Chesapeake Bay Water Quality Monitoring
Program Long-term benthic monitoring and assessment component. July 1984-Dec 1997.
Versar, Inc., Columbia, MD.
- 780
- 782 Rigaud, S., Puigcorbé, V., Camara-Mor, P., Casacuberta, N., Roca-Martí, M., Garcia-Orellana, J.,
Benitez-Nelson, C.R., Masque, P., Church, T. submitted, 2013. An assessment of the methods,
calculation and uncertainties in the determination of ^{210}Po and ^{210}Pb activities in
784 seawater. *Limnol. Oceanogr. Methods*.
- 786 Rutgers van Der Loeff, M. M., Moore, W.S., 2007. Determination of natural radioactive
tracers, p. 365-397, in: *Methods of Seawater Analysis*. Wiley-VCH Verlag GmbH.
- 788
- 790 Santschi, P.H., Li, Y.H., Bell, J., 1979. Natural radionuclides in the water of Narragansett Bay.
Earth Planet. Sci. Lett., 45, 201-213.
- 792 Sarin, M. M., Bhushan, R., Rengarajan, R., Yadav, D.N.. 1992. The simultaneous determination
of ^{238}U series nuclides in seawater: results from the Arabian Sea and Bay of Bengal. *Indian*
794 *J. Mar. Sci.* 21, 121-127.
- 796 Schlitzer, R., 2013. Ocean Data View, <http://odv.awi.de>.

798 Sharp, J. Coulberson, C. Church, T., 1982. The chemistry of the Delaware estuary. General
 Considerations. *Limnol. Oceanogr.*, 27(6), 1015-1028.

800 Smoak, J.M., DeMaster, D.J., Kuehl, S.A., Pope, R.H., McKee, B.A., 1996. The behavior of
 802 particle-reactive tracers in a high turbidity environment: ^{234}Th and ^{210}Pb on the Amazon
 continental shelf. *Geochimica et Cosmochimica Acta* 12, 2123–2137.

804 Stewart, G., Cochran, J., Xue, J., Lee, C., Wakeham, S., Armstrong, R., Masque, P., Miquel, J.
 2007. Exploring the connection between ^{210}Po and organic matter in the northwestern
 806 Mediterranean. *Deep Sea Research I.* 54, 415-427.

808 Stewart G.M. and Fisher, N.S. 2003a. Experimental Studies on the accumulation of polonium-
 210 by marine phytoplankton. *Limnology and Oceanography.* 48(3): 1192-1201.

810 Stewart, G., Fowler, S., and Fisher, N. 2007. Chapter 8: The Bioaccumulation of U- and Th-
 812 Series Radionuclides in Marine Organisms. *Radioactivity in the Environment, Volume 13.*

814 Stumm, W., Morgan, J.J., 1981. *Aquatic Chemistry.* Wiley, New York, 780 pp.

Thomson, J., Turekian, K.K., 1976. ^{210}Po and ^{210}Pb distributions in ocean water profiles
 816 from the Eastern South Pacific. *Earth Planet. Sci. Lett* 32, 297-303.

818 Todd, J.F., Wong, G.T.F., Reid, D., 1986. The geochemistries of ^{210}Po and ^{210}Pb in waters
 overlying and within the Orca Basin, Gulf of Mexico. *Deep Sea Res.* 33, 1293-1306.

820 Voynova, Y. and Sharp, J. 2012. Anomalous Biogeochemical Response to a Flooding Event in
 822 the Delaware Estuary: A Possible Typology Shift Due to Climate Change. *Estuaries and
 Coasts* 35:943-958.

824 Wei, C, and Murray, J. 1993. The behavior of scavenged isotopes in marine anoxic
 826 environments: ^{210}Pb and ^{210}Po in the water column of the Black Sea. *Geochmica et
 Cosmochimica Acta*, Vol. 58, No. 7, 1795-1811.

828

830

832

834

836

838

Table and Figure Captions

840

842 **Table 1:** Dissolved and particulate ^{210}Po and ^{210}Pb activities (dpm/100L) for the Delaware Bay (DB) and salt marsh (DBSMS), and Chesapeake Bay (CB).

844 **Table 2:** Dissolved ^{210}Po and ^{210}Pb activities (dpm/100L) for Roosevelt Inlet (RI) and Canary Creek (CC) lower Delaware Bay salt marsh.

846

848 **Table 3:** Box model units, rates, and residence times for the Delaware Bay and upper Chesapeake Bay estuaries

850 **Figure 1:** Location of the sampling sites in the Delaware Bay and Chesapeake Bay estuaries. The dashed line delineates the regions modeled. Samples were collected as follows: Delaware estuary 2012 April 1-3, Delaware salt marsh two locations over a 12hr tidal cycle 2012 June 1, and Chesapeake estuary 2012 August 20-25. The shaded area denotes deeper estuarine basins.

856 **Figure 2:** Distribution of dissolved and particulate ^{210}Po and ^{210}Pb activities (dpm/100L) and $^{210}\text{Po}/^{210}\text{Pb}$ activity ratios distribution in the Delaware Bay estuary. Contour plots were carried out using the DIVA gridding tool of Ocean Data View software. Dashed lines delineate the regions modeled (upper, mid and lower estuary).

860

862 **Figure 3:** Dissolved ^{210}Po , ^{210}Pb activities (dpm/100L) and $^{210}\text{Po}/^{210}\text{Pb}$ activity ratios in Roosevelt inlet and Canary Creek over a 12-hr tidal cycle.

864 **Figure 4:** Distribution of dissolved and particulate ^{210}Po and ^{210}Pb activities (dpm/100L) and $^{210}\text{Po}/^{210}\text{Pb}$ activity ratios distribution in the upper Chesapeake Bay estuary. Contour plots were carried out using the DIVA gridding tool of Ocean Data View software. Dashed lines delineate the regions modeled (upper, mid and lower estuary).

868

870 **Figure 5:** Box model depiction and symbol notation for dissolved ^{210}Po in the Delaware Bay and upper Chesapeake Bay estuary. The Delaware Bay utilized a regional (3 box-model) estuary model, while the Chesapeake used a single box model for the entire upper estuary.

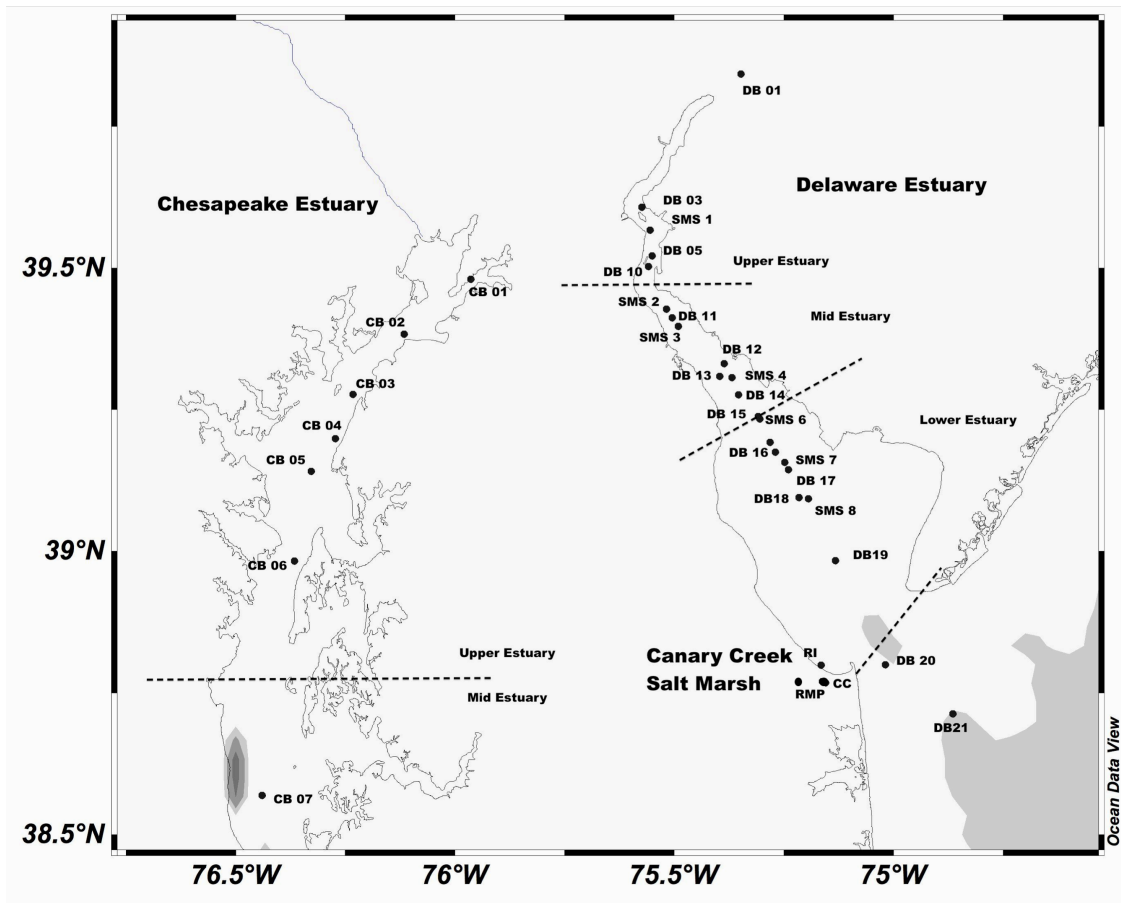
874

876

878

880

882



886 Figure 1

888

890

892

894

896

898

900

902

904

Table 1

Station	Salinity (psu)	Oxygen ($\mu\text{mol/L}$)	Depth (m)	$^{210}\text{Po}_{\text{diss}}$ (dpm/100L)	$^{210}\text{Po}_{\text{part}}$ (dpm/100L)	$^{210}\text{Pb}_{\text{diss}}$ (dpm/100L)	$^{210}\text{Pb}_{\text{part}}$ (dpm/100L)	$^{210}\text{Po}/^{210}\text{Pb}_{\text{diss}}$	$^{210}\text{Po}/^{210}\text{Pb}_{\text{part}}$
DB 01	0.1	323	11.8	1.8 ± 0.2	1.2 ± 0.7	1.9 ± 0.3	13.1 ± 1.6	0.9 ± 0.2	0.1 ± 0.0
DB 01	0.1	325	2.4	1.4 ± 0.2	1.3 ± 1.1	2.2 ± 0.4	15.2 ± 2.1	0.7 ± 0.1	0.1 ± 0.0
DB 03	2.0	319	10.4	1.6 ± 0.1	4.7 ± 1.0	3.0 ± 0.2	16.7 ± 2.0	0.5 ± 0.1	0.3 ± 0.1
DB 03	2.0	321	2.8	1.7 ± 0.2	4.8 ± 1.0	3.2 ± 0.4	16.8 ± 2.1	0.5 ± 0.1	0.3 ± 0.1
DB 05	7.2	320	2.0	2.6 ± 0.2	18.4 ± 1.9	1.4 ± 0.3	15.9 ± 3.2	1.9 ± 0.4	1.2 ± 0.3
DB 10	6.7	327	1.8	1.9 ± 0.2	14.8 ± 2.0	2.1 ± 0.3	57.8 ± 5.0	0.9 ± 0.2	0.3 ± 0.1
DB 10	8.5	319	9.1	2.0 ± 0.2	15.4 ± 1.0	2.1 ± 0.4	60.1 ± 4.9	0.9 ± 0.2	0.3 ± 0.1
DB 11	8.2	337	2.0	2.3 ± 0.2	4.9 ± 1.7	3.2 ± 0.4	9.1 ± 2.7	0.7 ± 0.1	0.5 ± 0.1
DB 11	12.4	315	10.0	2.0 ± 0.2	6.0 ± 1.0	1.7 ± 0.3	14.7 ± 2.9	1.2 ± 0.2	0.4 ± 0.1
DB 12	16.5	315	12.9	2.5 ± 0.2	11.0 ± 1.7	3.8 ± 0.4	20.1 ± 2.0	0.7 ± 0.1	0.5 ± 0.2
DB 12	10.9	342	2.2	1.8 ± 0.2	8.4 ± 2.6	1.0 ± 0.3	10.8 ± 2.9	1.8 ± 0.6	0.8 ± 0.2
DB 13	12.3	353	2.2	2.2 ± 0.2	6.8 ± 1.3	1.3 ± 0.3	10.7 ± 2.4	1.7 ± 0.4	0.6 ± 0.2
DB 13	15.4	300	10.1	2.3 ± 0.2	13.1 ± 1.5	1.3 ± 0.3	14.4 ± 2.8	1.8 ± 0.5	0.9 ± 0.2
DB 14	21.5	308	2.1	2.5 ± 0.2	16.1 ± 2.3	1.6 ± 0.3	14.5 ± 3.0	1.6 ± 0.3	1.1 ± 0.2
DB 14	16.2	347	15.4	2.2 ± 0.2	13.3 ± 2.6	2.4 ± 0.3	14.1 ± 4.3	0.9 ± 0.2	0.9 ± 0.3
DB 15	18.8	330	2.0	4.7 ± 0.4	4.0 ± 1.0	3.9 ± 0.4	0.6 ± 0.3	1.2 ± 0.2	6.8 ± 2.3
DB 15	23.7	307	14.3	2.1 ± 0.2	2.1 ± 0.9	2.0 ± 0.3	0.6 ± 0.3	1.1 ± 0.2	3.9 ± 1.4
DB 16	25.5	306	2.1	3.9 ± 0.3	1.8 ± 0.9	2.8 ± 0.3	0.4 ± 0.3	1.4 ± 0.2	4.5 ± 1.2
DB 16	21.5	318	11.7	2.6 ± 0.2	1.4 ± 1.1	1.6 ± 0.3	1.2 ± 0.9	1.6 ± 0.3	1.2 ± 0.8
DB 17	24.1	310	1.9	3.2 ± 0.3	1.6 ± 1.0	3.1 ± 0.4	0.5 ± 0.3	1.0 ± 0.2	3.2 ± 1.0
DB 17	26.0	301	12.1	3.4 ± 0.3	2.1 ± 0.9	2.9 ± 0.4	0.6 ± 0.3	1.2 ± 0.2	3.5 ± 1.1
DB 18	26.3	306	2.0	4.5 ± 0.4	3.4 ± 1.4	2.2 ± 0.3	1.2 ± 1.0	2.1 ± 0.3	2.7 ± 0.8
DB 19	28.2	297	2.0	3.3 ± 0.3	4.4 ± 1.2	1.6 ± 0.3	2.1 ± 1.3	2.0 ± 0.4	2.1 ± 1.5
DB 20	31.8	297	1.6	2.5 ± 0.2	1.6 ± 0.8	2.2 ± 0.3	2.4 ± 1.2	1.1 ± 0.2	0.6 ± 0.3
DB 21	30.4	295	2.0	2.2 ± 0.2	2.3 ± 1.3	1.8 ± 0.2	2.4 ± 2.0	1.3 ± 0.1	1.0 ± 0.3
DB 21	31.0	292	15.3	2.7 ± 0.2	1.1 ± 0.4	1.2 ± 0.3	1.0 ± 0.4	2.2 ± 0.5	1.1 ± 0.3
DBSMS 1	5.2	326	2.0	1.5 ± 0.2	15.1 ± 1.8	1.3 ± 0.3	14.2 ± 2.3	1.1 ± 0.3	1.1 ± 0.1
DBSMS 2	10.3	323	2.0	2.0 ± 0.2	9.1 ± 2.2	1.6 ± 0.3	14.0 ± 2.5	1.2 ± 0.3	0.7 ± 0.2
DBSMS 3	13.2	315	2.0	2.4 ± 0.2	10.0 ± 2.0	1.3 ± 0.3	11.8 ± 1.8	1.9 ± 0.5	0.9 ± 0.2
DBSMS 4	15.1	311	2.0	1.3 ± 0.2	7.5 ± 1.3	1.0 ± 0.3	10.5 ± 2.5	1.3 ± 0.4	0.7 ± 0.3
DBSMS 5	17.6	308	2.0	2.5 ± 0.3	3.7 ± 1.1	3.8 ± 0.5	0.8 ± 0.2	0.6 ± 0.1	4.8 ± 1.9
DBSMS 6	21.2	303	2.0	1.5 ± 0.2	1.4 ± 0.9	1.7 ± 0.3	0.8 ± 0.4	0.9 ± 0.2	1.8 ± 0.6
DBSMS 7	23.3	302	2.0	4.3 ± 0.3	1.7 ± 0.9	2.1 ± 0.4	0.6 ± 0.2	2.0 ± 0.4	2.9 ± 1.0
DBSMS 8	25.9	301	2.0	3.9 ± 0.3	3.3 ± 1.2	2.0 ± 0.3	1.4 ± 0.9	2.0 ± 0.4	2.4 ± 1.0
CB 01	12.7	188	4.8	2.1 ± 0.2	0.8 ± 0.1	1.2 ± 0.3	1.8 ± 0.3	1.8 ± 0.5	0.4 ± 0.1
CB 01	14.2	130	10.4	1.4 ± 0.2	0.5 ± 0.2	0.6 ± 0.3	3.1 ± 0.5	2.2 ± 1.1	0.2 ± 0.1
CB 01	15.9	34	17.7	2.8 ± 0.2	0.5 ± 0.2	0.9 ± 0.3	1.0 ± 0.4	3.2 ± 1.2	0.5 ± 0.2
CB 01	17.1	2	22.0	2.2 ± 0.2	1.3 ± 0.1	0.7 ± 0.3	0.7 ± 0.3	3.0 ± 1.2	1.8 ± 0.5
CB 02	13.1	153	3.0	1.5 ± 0.2	2.4 ± 0.1	0.6 ± 0.3	0.7 ± 0.3	2.5 ± 1.2	3.5 ± 1.4
CB 02	14.2	71	8.2	4.4 ± 0.4	5.3 ± 0.1	3.0 ± 0.5	1.9 ± 0.3	1.5 ± 0.3	2.8 ± 0.1
CB 02	15.5	41	13.9	2.7 ± 0.3	10.7 ± 0.2	1.0 ± 0.5	67.1 ± 0.9	2.6 ± 1.3	0.2 ± 0.6
CB 02	17.0	1	21.9	1.1 ± 0.2	2.6 ± 0.1	4.3 ± 1.0	0.3 ± 0.2	0.2 ± 0.1	8.3 ± 2.5
CB 02	17.0	1	21.5	1.3 ± 0.3	1.6 ± 0.2	0.4 ± 0.3	0.4 ± 0.2	3.2 ± 2.7	4.3 ± 1.8
CB 03	10.8	142	0.8	1.6 ± 0.2	0.3 ± 0.1	2.7 ± 0.4	1.9 ± 0.1	0.6 ± 0.1	0.2 ± 0.0
CB 03	13.3	23	9.1	2.5 ± 0.2	6.9 ± 0.1	0.5 ± 0.3	2.8 ± 0.2	4.7 ± 2.7	2.5 ± 0.2
CB 04	8.0	188	1.1	1.4 ± 0.2	5.5 ± 0.1	0.7 ± 0.3	1.8 ± 0.2	2.0 ± 0.9	3.1 ± 0.3
CB 05	6.6	177	1.9	2.0 ± 0.3	3.3 ± 0.1	2.4 ± 0.5	3.3 ± 0.2	0.8 ± 0.2	1.0 ± 0.1
CB 05	10.0	96	9.1	2.0 ± 0.3	9.6 ± 0.1	0.9 ± 0.5	10.7 ± 0.2	2.1 ± 1.1	0.9 ± 0.0
CB 06	3.2	175	0.5	0.8 ± 0.2	10.0 ± 0.2	0.4 ± 0.3	7.6 ± 0.3	1.9 ± 1.3	1.3 ± 0.1
CB 07	2.1	172	0.5	2.6 ± 0.4	3.5 ± 0.2	1.1 ± 0.5	34.8 ± 0.5	2.3 ± 1.1	0.1 ± 0.0
CB 07	3.1	155	9.0	2.1 ± 0.2	31.3 ± 0.6	0.9 ± 0.3	27.6 ± 0.7	2.3 ± 0.9	1.1 ± 0.0

DB: Delaware Bay Stations DBSMS: Delaware Bay Surface Mapping System
 CB: Chesapeake Bay Stations

914

916 **Table 2:**

Station	Salinity (psu)	Tide Height	²¹⁰ Po _{diss} (dpm/100L)		²¹⁰ Pb _{diss} (dpm/100L)		²¹⁰ Po/ ²¹⁰ Pb _{diss}	
RI 01	26.8	high tide	4.3	± 0.3	1.7	± 0.4	2.5	± 0.5
RI 02	27.4	ebbing	3.5	± 0.3	1.2	± 0.4	2.8	± 0.5
RI 03	27.6	ebbing	5.8	± 0.5	3.8	± 0.4	1.5	± 0.2
RI 04	27.4	ebbing	2.8	± 0.2	1.9	± 0.4	1.5	± 0.3
RI 05	25.8	low tide	9.9	± 0.8	11.6	± 1.1	0.9	± 0.1
RI 06	25.7	flooding	5.0	± 0.4	4.2	± 0.5	1.2	± 0.2
RI 07	27.9	flooding	3.5	± 0.3	2.5	± 0.5	1.4	± 0.3
RI 08	28.1	flooding	3.3	± 0.3	2.6	± 0.7	1.2	± 0.4
CC 01	21.7	high tide	6.7	± 0.6	6.4	± 0.7	1.0	± 0.1
CC 02	23.2	ebbing	3.9	± 0.4	7.2	± 0.8	0.5	± 0.1
CC 03	21.2	ebbing	6.1	± 0.7	6.4	± 0.7	1.0	± 0.2
CC 04	20.2	ebbing	6.7	± 1.1	13.8	± 1.5	0.5	± 0.1
CC 05	19.5	low tide	4.8	± 0.7	5.5	± 0.7	0.9	± 0.2
CC 06	18.2	flooding	8.3	± 0.7	4.6	± 0.6	1.8	± 0.3
CC 07	19.3	flooding	10.1	± 0.9	8.7	± 0.9	1.2	± 0.2
CC 08	20.5	flooding	13.9	± 1.0	6.0	± 0.7	2.3	± 0.3
RMP	0.4	low tide	9.0	± 1.4	18.8	± 2.5	0.5	± 0.1

RI: Roosevelt Inlet Marsh RMP: Red Mill Pond end member
 CC: Canary Creek Marsh

918

920

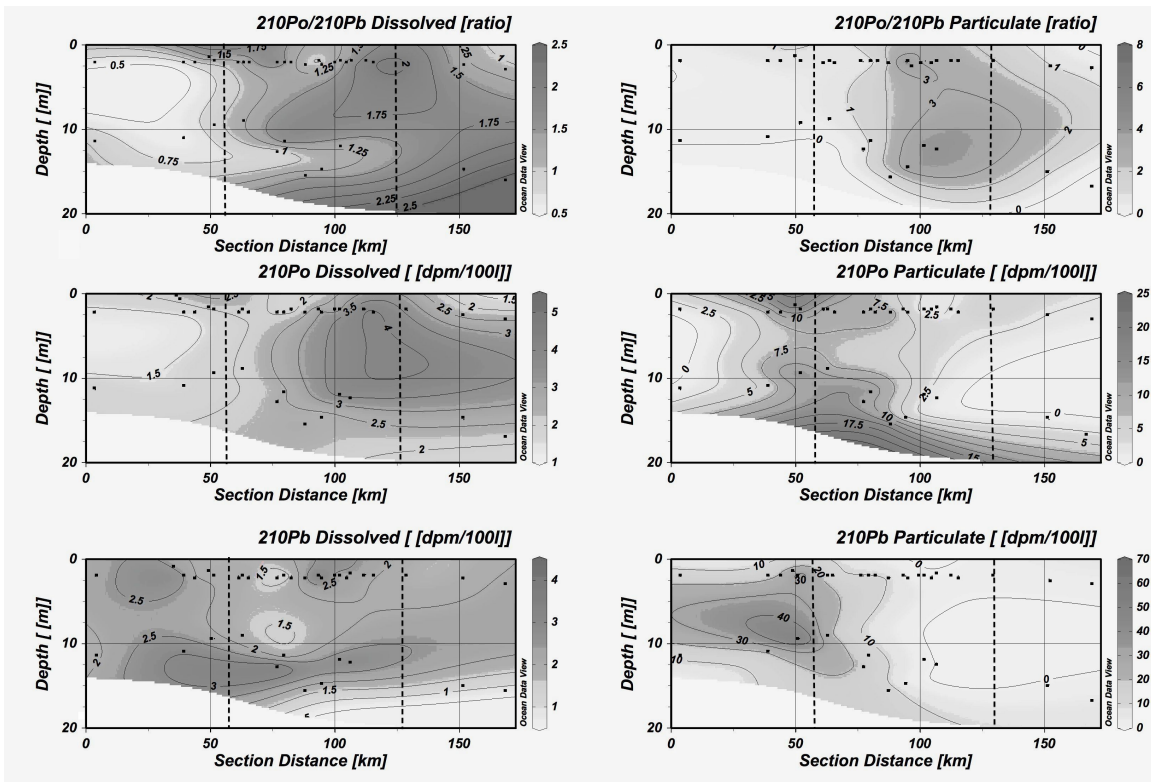
922

924

926

928

930



932

Figure 2

934

936

938

940

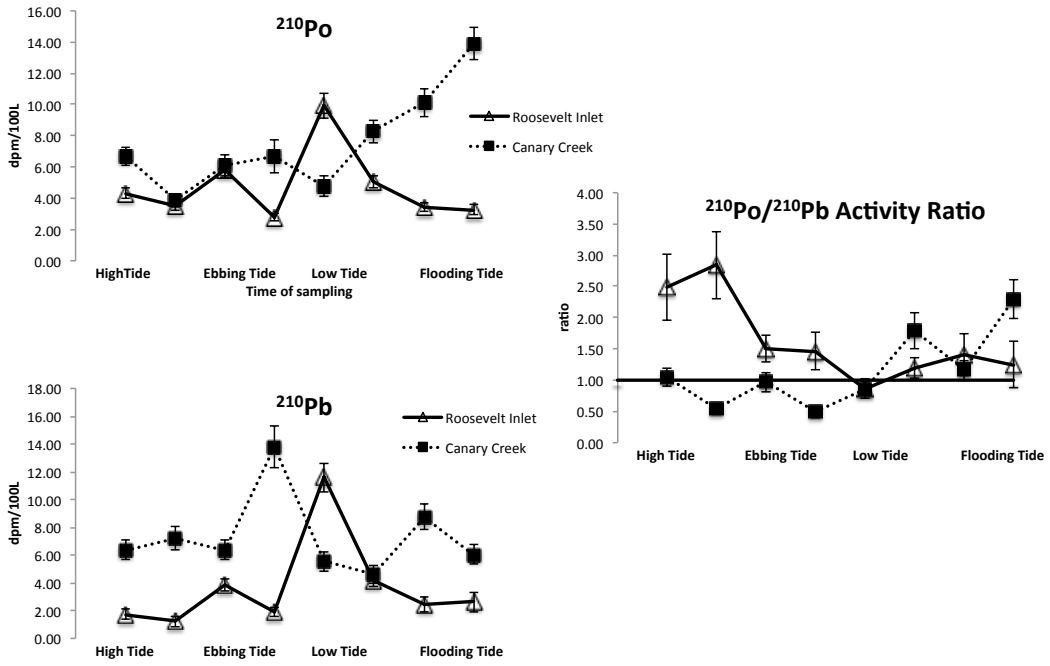
942

944

946

948

950

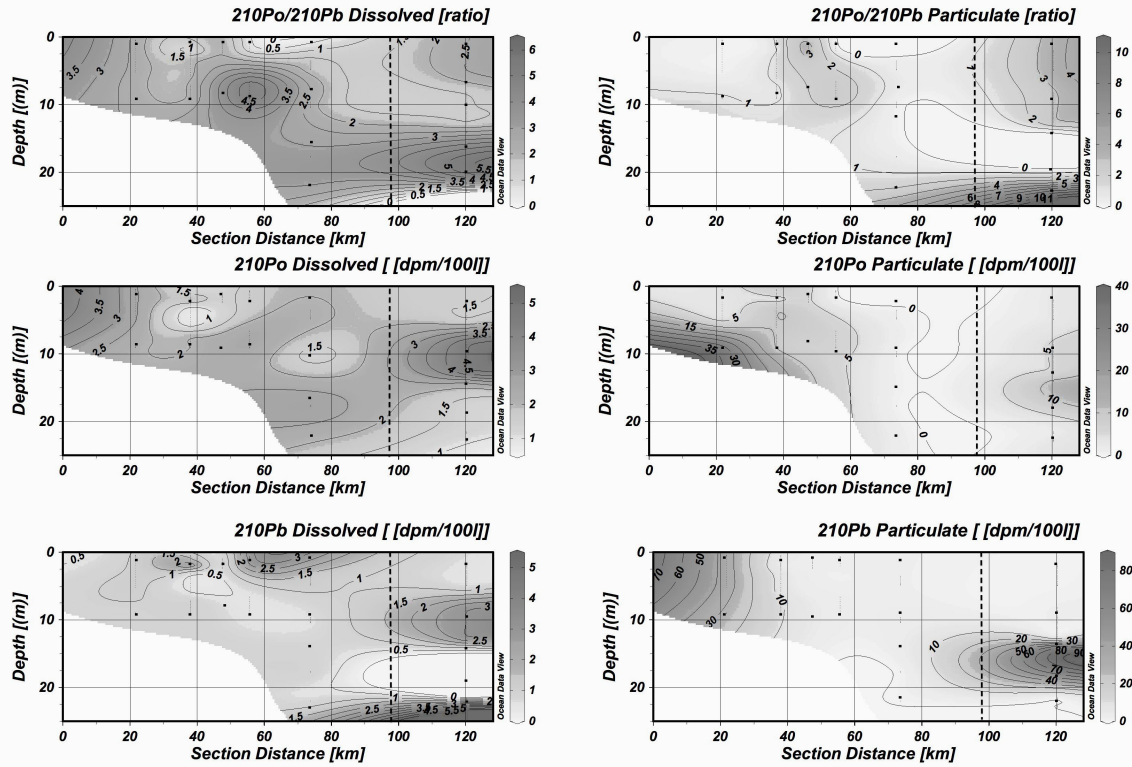


952

Figure 3

954

956



958 **Figure 4**

960

962

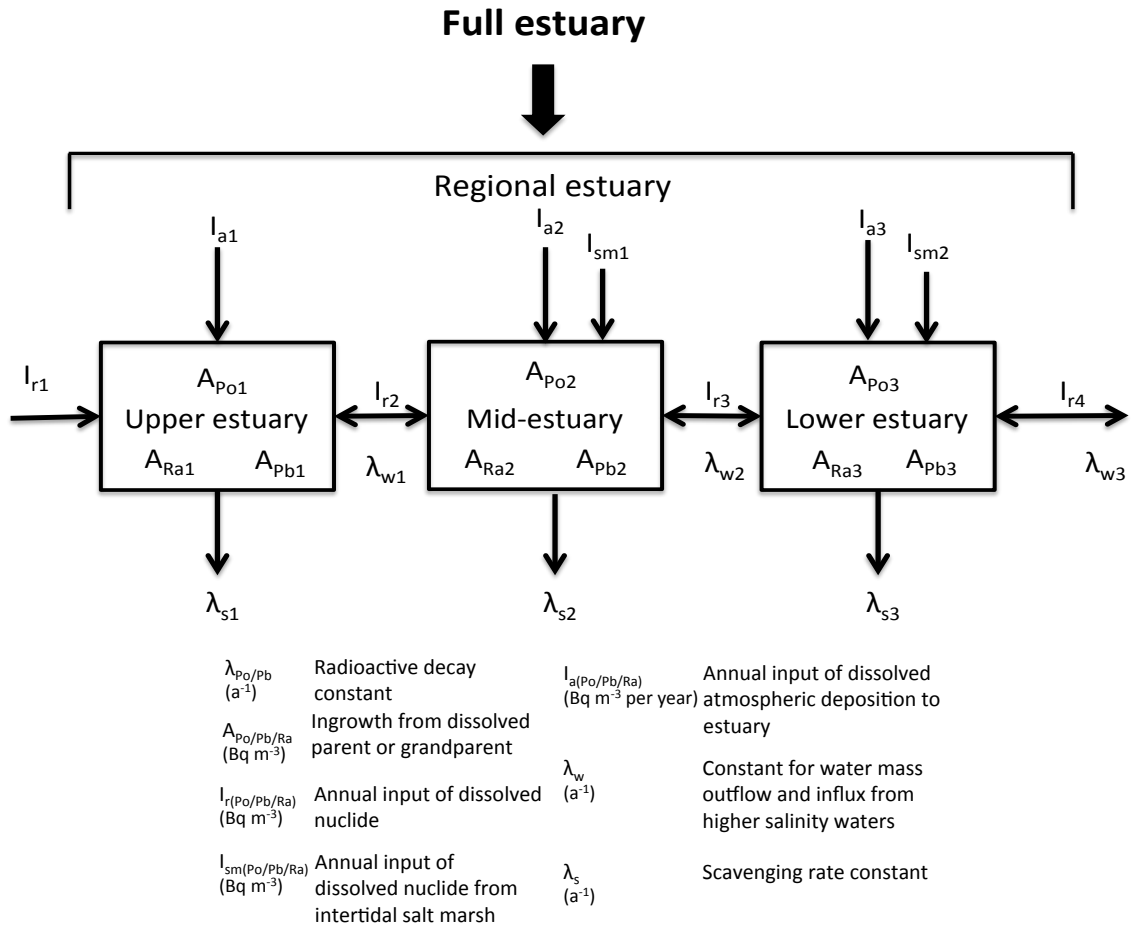
964

966

968

970

972



974

Figure 5

976

978

980

982

984

986

988

Table 3

	$\lambda(a^{-1})$	A(dpm/100L)	I _i (dpm/100L)	I _{sm} (dpm/100L)	I _a (dpm/100L/a ¹)	$\lambda_e(a^{-1})$	$\lambda_w(a^{-1})$	Residence Time (d)
		240 (²¹⁰ Po)	480 (²¹⁰ Po)	480 (²¹⁰ Po)				
	1.8 (²¹⁰ Po)	180 (²¹⁰ Pb)	240 (²¹⁰ Pb)	780 (²¹⁰ Pb)	1.3x10 ⁻⁵ (²¹⁰ Po)	4.2 (²¹⁰ Po)		87 (²¹⁰ Po)
Delaware	3.1x10 ⁻² (²¹⁰ Pb)	540 (²²⁶ Ra)	180 (²²⁶ Ra)	1080 (²²⁶ Ra)	1.3x10 ⁻³ (²¹⁰ Pb)	5.5 (²¹⁰ Pb)	2.9	66 (²¹⁰ Pb)
		180 (²¹⁰ Po)	240 (²¹⁰ Po)					
	1.8 (²¹⁰ Po)	120 (²¹⁰ Pb)	120 (²¹⁰ Pb)		1.3x10 ⁻⁵ (²¹⁰ Po)	2.9 (²¹⁰ Po)		126 (²¹⁰ Po)
Chesapeake	3.1x10 ⁻² (²¹⁰ Pb)	1860 (²²⁶ Ra)	600 (²²⁶ Ra)	-	1.3x10 ⁻³ (²¹⁰ Pb)	6.6 (²¹⁰ Pb)	1.0	53 (²¹⁰ Pb)

990

992